

Deflagration-to-Detonation Transition Tests in $\text{H}_2\text{-O}_2\text{-N}_2\text{-He}$ Mixtures

Z. Liang, J. Karnesky and J. E. Shepherd

Graduate Aeronautical Laboratories
California Institute of Technology
Pasadena, CA 91125

Explosion Dynamics Laboratory Report FM2006.004

August 29, 2006

Prepared for Los Alamos National Laboratory

1 Introduction

The purpose of the present study is to evaluate the threshold for deflagration-to-detonation transition (DDT) inside of a vessel containing a hydrogen-oxygen-nitrogen-helium mixture. These are preliminary tests intending to provide scoping data on the possibility of DDT in the inner vessel of the triple-nested containers used in the DOE complex for PuO_2 storage. The dimensions of the test vessel do not match the dimensions of the actual containers and the results of the present study are intended to guide future, more realistic, testing. A thick-wall test vessel was used and although strain was measured in some tests, no attempt was made to mimic the construction or structural response of the actual containers.

A series of 26 tests were carried out in a test vessel (3 in inside diameter, 14 in long), closed at both ends and instrumented with pressure and strain gauges. The test mixture was 40.9 % hydrogen, 22.4 % oxygen, 7.7 % nitrogen and 29 % helium at the initial pressure P_0 equal to 2.0 – 2.35 bar. DDT transition was observed when P_0 was increased to 2.3 – 2.35 bar, below which, slow flame was observed.

2 Experimental Set-up

The vessel was constructed with 1-in thick welded flanges and bolted closures on the ignition side (see Fig. 1). The vessel has a length of 14 in as measured between the inner surfaces of the flanges, a tube inner diameter of 3 in, and the tube wall thickness was 0.25 in .

The mixture was ignited by a glow plug which was mounted in the center of the right flange. One piezoelectric pressure transducer (PCB) was mounted on the left end wall. Model 113A26 (dynamic range of 7 MPa) was used for shot 2; model 113A24 (a dynamic range of 14 MPa) was used for shot 3 and 4 used; for the rest, model 113A23 (a dynamic range of 140 MPa) was used.

After the initial 10 shots, four strain gauges were mounted on the outer tube surface close to the reflecting end wall (see Fig.1b). The strain gauges are of type CEA-06-125UN-350. The gauges are operated with an excitation voltage of 10 V in the quarter bridge mode using the built-in 350 Ω dummy gauges of the signal conditioning amplifiers (Type 2310A, Vishay Measurements Group, Micro-Measurements Division). An amplification factor of 500 for the strain gauge signals was used. The bridge circuits are balanced prior to the ignition event.

3 Experimental Results

All tests were carried out at the initial conditions of room temperature, 22-25°C, and an initial pressure of 2.0-2.3 bar. The fuel was a mixture of 40.9 % hydrogen, 22.4 % oxygen, 7.7 % nitrogen and 29 % helium.

The pressure and strain signals were analyzed using computed values of the peak pressure for idealized combustion processes. The values for CJ pressure (P_{CJ}), reflected CJ pressure (P_{CJref}) and constant volume explosion pressure (P_{CV}) are calculated using a chemical equilibrium program of STANJAN. The CJ detonation pressure is similar for all of the shots and is approximately 3.7-4.3 MPa, with reflected detonation pressure of approximately 9.1-

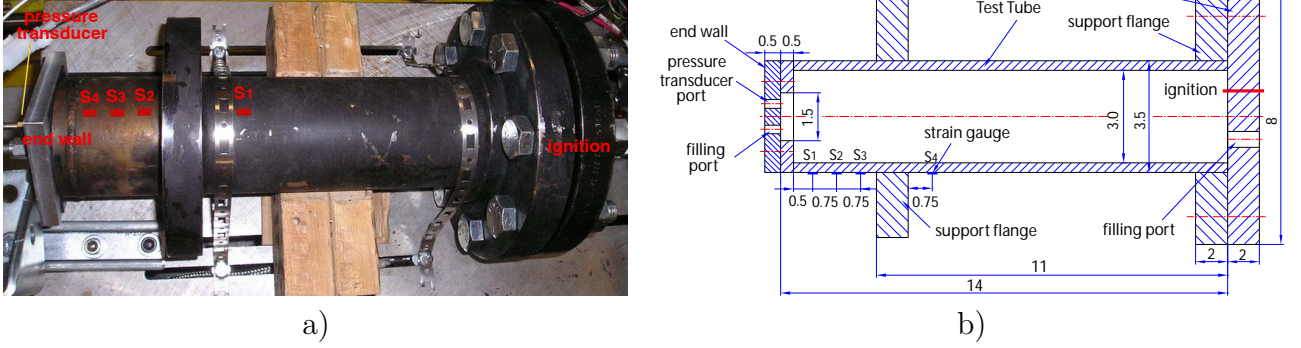


Figure 1: Experimental setup. Ignition flange is to the right. One pressure transducer is on the left. Four strain gauges were added after the first 10 shots.

10.8 MPa. The experimental peaks P_{max} and ϵ_{max} are the maximum measured pressure and maximum strain recorded on the strain gauges (S₁-S₄), respectively.

The location of DDT onset was determined by examining the pressure traces for the characteristic signatures of DDT. Near the DDT location, the pressure peak will have a sharp front and a value several times higher than the CJ pressure P_{CJ} . The DDT event produces strong shock waves in the burned gas that can be observed as sharp jumps in the pressure signals that propagate away from the DDT location. DDT events also produce structural oscillations, including flexural waves, that create very distinctive high frequency signals in the strain gauges. The results for all tests are summarized in Table 1 and Fig. 2. The pressure trace and strain gauges are attached in the end of the report.

In the first ten shots (1-10), only pressure signals were recorded. For $P_0 = 2.3$ bar, the onset of detonation is near the end wall and occurs after the reflection of a series of shock waves generated by the high speed deflagration that proceeded the detonation (see Figs. 5b-f). The peak pressure recorded in shot 5 is 4 times larger than P_{CJref} . When $P_0 < 2.3$ bar, slow combustion was observed (see Figs. 6 and 7).

Shots 11-26 are repetitions of two initial conditions: $P_0 = 2.3$ and 2.35 bar. For $P_0 = 2.3$ bar, DDT events appeared in shots 13, 14 and 15 (Figs. 8c, d, e). The maximum pressure of shot 13 is 43.34 MPa and the peak strain is 218 μ strain. The peak pressures of shot 14 and 15 are all much smaller than shot 13, but they are comparable with P_{CJ} . Also the presence of high-amplitude and high-frequency oscillations in the strain signals (Figs. 14 and 15) combined with spikes in the pressure signals indicates (Figs. 8d and e) that DDT took place. We think the DDT transition appeared somewhere in the tube before the deflagration wave reached the end wall. For $P_0 = 2.35$ bar, DDT events were observed in shots 17 and 21. The huge pressure spike, 90 MPa, recorded in shot 21, is mainly due to recessing of the pressure transducer from the reflecting surface (0.1 in away from the end wall) and the presence of the 0.5-in welded flange on the left end of the tube with a smaller hole inner diameter (1.5 in).

Table 1: Summary of all shots in the 40.9% H_2 -22.4% O_2 -7.7% N_2 -29% He mixture.

shot	P_0 (MPa)	P_{CV} (MPa)	P_{CJ} (MPa)	P_{CJref} (MPa)	P_{max} (MPa)	ϵ_{max} (μstrain)	Φ_{exp}	Mode
7	0.20	1.902	3.724	9.131	2.013	—	—	flame
8	0.20	1.902	3.724	9.131	1.825	—	—	flame
10	0.22	2.099	4.108	10.076	2.746	—	—	flame
9	0.215	2.049	4.012	9.839	2.285	—	—	flame
1	0.23	2.197	4.301	10.548	2.66	—	—	flame
2	0.23	2.197	4.301	10.548	7.137 ¹	—	—	DDT
3	0.23	2.197	4.301	10.548	13.856 ¹	—	—	DDT
4	0.23	2.197	4.301	10.548	13.856 ¹	—	—	DDT
5	0.23	2.197	4.301	10.548	7.641	—	—	DDT
6	0.23	2.197	4.301	10.548	40.235	—	—	DDT
11	0.23	2.197	4.301	10.548	3.05	77	0.815	flame
12	0.23	2.197	4.301	10.548	2.68	75	0.904	flame
13	0.23	2.197	4.301	10.548	43.34	218	0.162	DDT
14	0.23	2.197	4.301	10.548	3.39	98	0.934	DDT
15	0.23	2.197	4.301	10.548	3.74	88	0.760	DDT
16	0.23	2.197	4.301	10.548	2.85	77	0.873	flame
17	0.235	2.246	4.398	10.785	42.13	171	0.131	DDT
18	0.235	2.246	4.398	10.785	3.03	79	0.842	flame
19	0.235	2.246	4.398	10.785	3.12	81	0.839	flame
20	0.235	2.246	4.398	10.785	3.05	83	0.879	flame
21	0.235	2.246	4.398	10.785	90.68	200	0.071	DDT
22	0.235	2.246	4.398	10.785	2.88	77	0.864	flame
23	0.235	2.246	4.398	10.785	3.05	80	0.847	flame
24	0.235	2.246	4.398	10.785	2.37	77	1.050	flame
25	0.235	2.246	4.398	10.785	3.26	80	0.793	flame
26	0.235	2.246	4.398	10.785	3.25	79	0.785	flame

3.1 Impulse of the reflected pressure waves

One of the methods used to characterize the pressure-time histories is to compute the impulse or area under the pressure-time curves. The signals from the pressure transducer have been analyzed and the impulses (see table 2) computed by numerically integrating (using the trapezoidal rule) the pressure signal over a time interval. Typically, the interval between the first and the second peak is close to 0.3-45 ms for all DDT shots (see an example of Fig 3), corresponding waves reverberating inside the tube with a speed of 1600-2370 m/s. Although the peak pressure in these spikes can be as high as 40 MPa, the duration is so short that the load is impulsive and only a small increment in deformation will be produced. For $P_0 = 2.3$ bar, the value of the impulse associated with the first pulse is 0.45 KPa·s and the impulse is

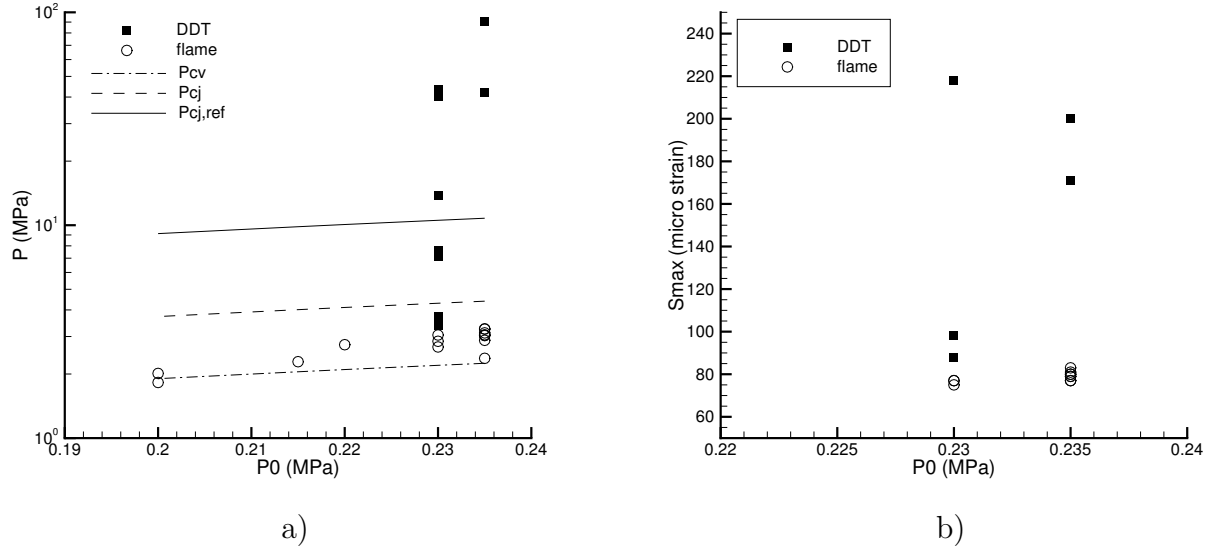


Figure 2: a) Peak pressure P_{max} and b) Peak strain ϵ_{max} vs. initial pressure P_0 .

7.3 KPa·s for a long (8 ms) integration time.

$$I = \int_{t_1}^{t_2} P(t) dt \quad (1)$$

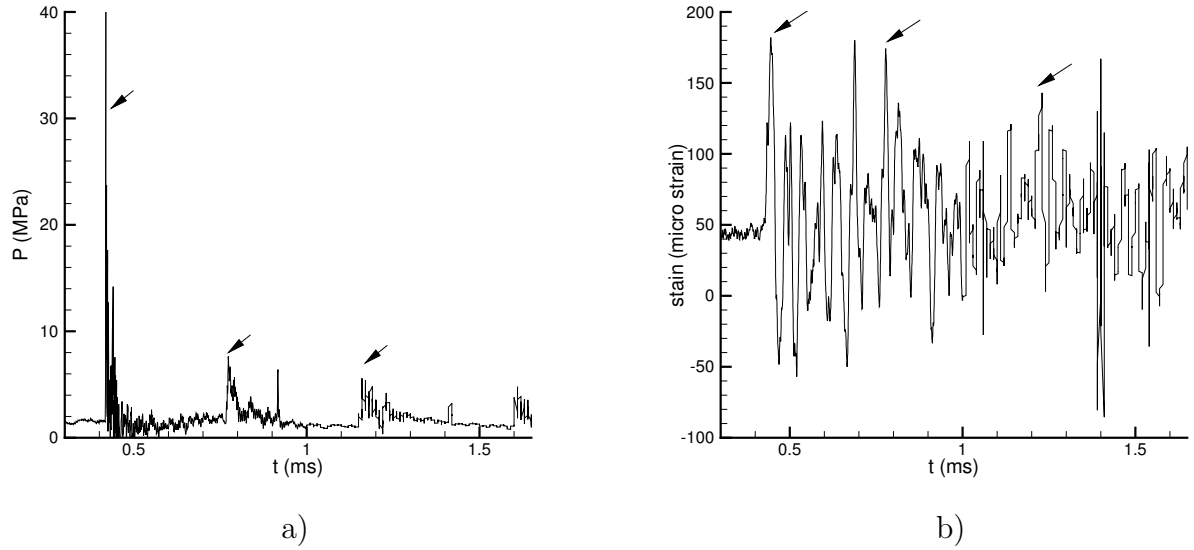


Figure 3: a) Pressure and b) strain gauge trace of shot 13 for $P_0 = 2.3$ bar. The arrows show the location of the peak pressure and the corresponding strain response.

Table 2: Impulse computed from the pressure measured on the reflecting end flange.

shot	P_0 (MPa)	I (kPa·s)	time period (t_1 - t_2 ms)	I (kPa·s)	time period (ms)
2	0.23	0.540	1.50-1.87	7.33	0-8
4	0.23	0.508	1.50-1.85	9.40	0-8
5	0.23	0.581	0.30-0.70	12.39	0-8
6	0.23	0.446	0.27-0.54	8.32	0-8
13	0.23	0.707	0.41-0.78	11.45	0-8
14	0.23	0.846	1.6-2.1	12.13	0-8
15	0.23	0.859	0.9-1.4	11.98	0-8
17	0.235	1.033	0.3-0.75	12.46	0-8
21	0.235	1.031	1.0-1.45	13.22	0-8

3.2 Dynamic load factor

The peak value of the strain signals can be analyzed by finding the dynamic load factor (DLF) Φ , which is defined as the ratio of the measured peak strain to the peak strain expected in the case of quasi-static loading with the peak pressure

$$\Phi = \frac{\epsilon_{max}}{\frac{\Delta PR}{Eh}} \quad (2)$$

where $E = 210$ GPa, $R = 1.625$ in (mean of inner and outer radius), $h = 0.25$ in. The dynamic load factors computed with Eq. 2 of shots 11-26 are summarized in Table 1. Φ_{exp} was computed based on the measured peak pressure P_{max} and ϵ_{max} . When DDT occurred, Φ_{exp} tends to be small because of the short duration of the pressure pulses.

The axi-symmetric radial vibrations of a long (axially unconfined) cylinder have a fundamental frequency of

$$f = \frac{1}{2\pi R} \sqrt{\frac{E}{\rho(1-\nu^2)}}, \quad (3)$$

where $\rho = 7.8 \cdot 10^3$ kg/m³, $\nu = 0.3$ which results in a frequency of $f = 22.7$ kHz, corresponding to an oscillation period of 44.0 μ s. The time required for elastic wave transit time through the thickness h is

$$\tau_{wave} = h/c_l \quad (4)$$

where the longitudinal sound speed $c_l = 6100$ m/s for steel, so that, $\tau_{wave} = 1.05$ s,

$$\tau_{wave} \ll T. \quad (5)$$

This circumstance greatly simplifies the mathematical treatment of thin cylinders and enables the computation of the peak strain by equating the initial kinetic energy \mathcal{K} and the peak strain energy \mathcal{S}_e

$$\mathcal{K} = \mathcal{S}_e, \quad \text{or} \quad \frac{I^2}{2\rho h} = \frac{1}{2} \frac{Eh}{1-\nu^2} \epsilon_{max}^2, \quad (6)$$

which shows that the peak strain depends linearly on the impulse in this limit

$$\epsilon_{max} = \sqrt{\frac{1 - \nu^2}{Eh^2\rho}} I . \quad (7)$$

For rectangular-pulse loading, this is

$$\epsilon_{max} = \sqrt{\frac{1 - \nu^2}{Eh^2\rho}} P_{max}\tau . \quad (8)$$

yielding a linear dependence of the maximum strain on the pulse duration τ for a fixed peak pressure P_{max} . Using the definition of dynamic load factor, Eq. 2 and the frequency of oscillation, Eq. 3, the dynamic load factor can be expressed analytically as

$$\Phi = 2\pi \frac{\tau}{T} , \quad \tau \leq 0.4T \quad (9)$$

As shown in Fig. 4 for shot 13, $\tau \approx 1.5 \mu s$ at $P = 35$ MPa, the expected Φ is 0.21 based on Eq. 9, which is close to the computed value 0.16 based on Eq. 2. Also according to Eq. 8, $\epsilon_{max} = 195 \mu strain$, which is similar to the measured value of 218 $\mu strain$.

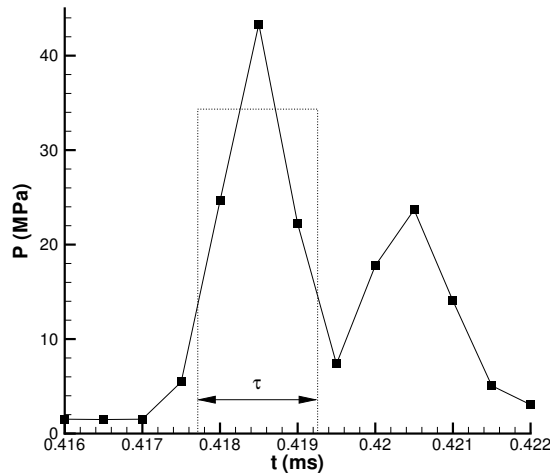


Figure 4: Pressure traces of shot 13 showing the first impulse, $\tau \approx 1.5 \mu s$ at $P = 35$ MPa.

4 Summary

A series of scoping tests have demonstrated that it is possible to obtain DDT in a cylinder with dimensions comparable to the convenience can of the nested can assembly used in the DOE complex for PuO_2 storage. The threshold of DDT for the mixture studied appears to occur at about 2.3-2.4 bar. Comparison of the peak strains and peak pressures using a dynamic load factor approach shows that the detonation loading is in the impulsive regime. These tests show that DDT may occur in this geometry. In order to fully assess the DDT hazard, further testing is required with fixtures that better simulate the convenience cans and the annular geometry between the inner and outer cans.

A Pressure Traces

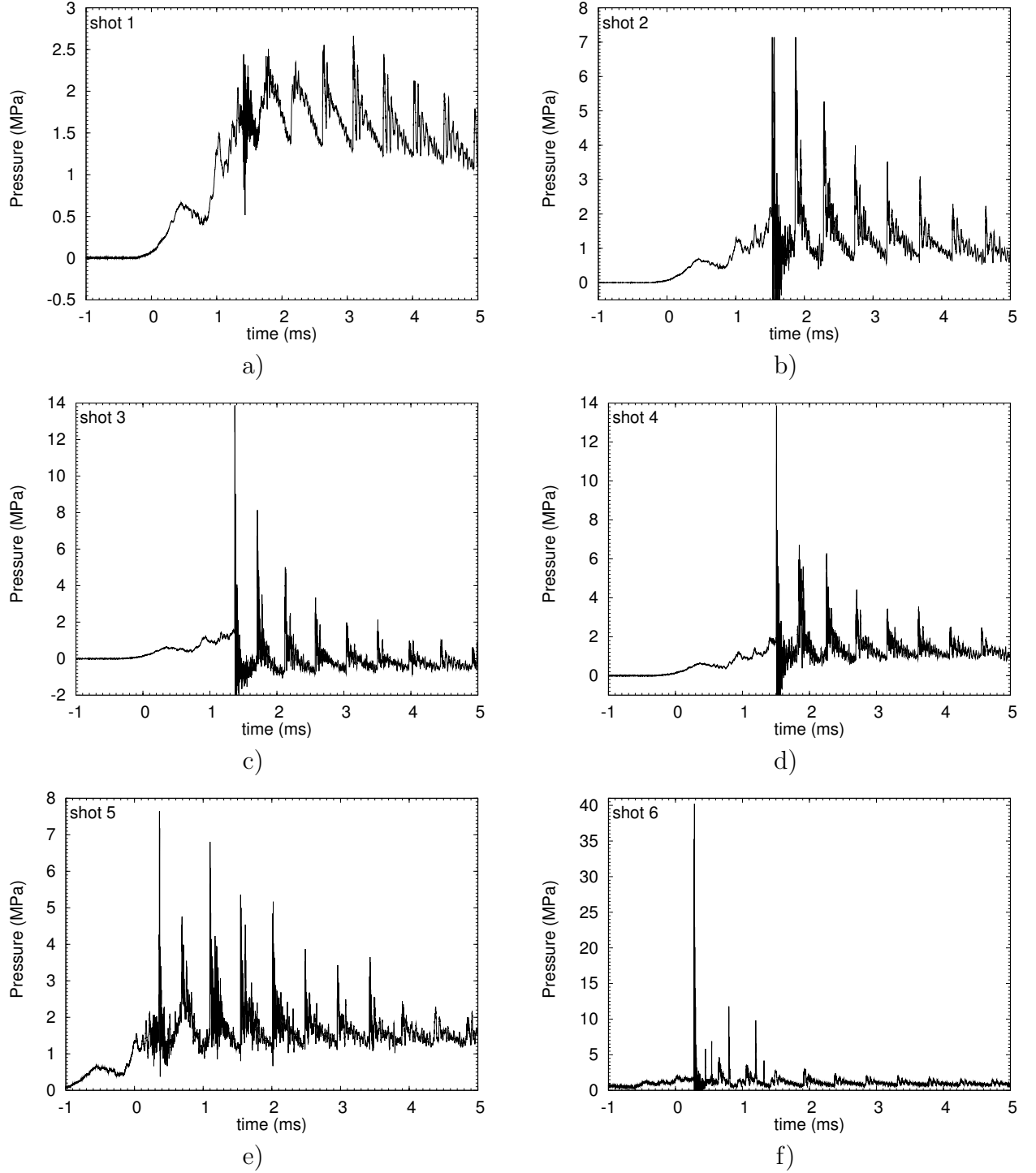


Figure 5: Pressure traces of a) shot 1, b) shot 2, c) shot 3, d) shot 4, e) shot 5 and f) shot 6 for $P_0 = 2.3$ bar without strain gauges.

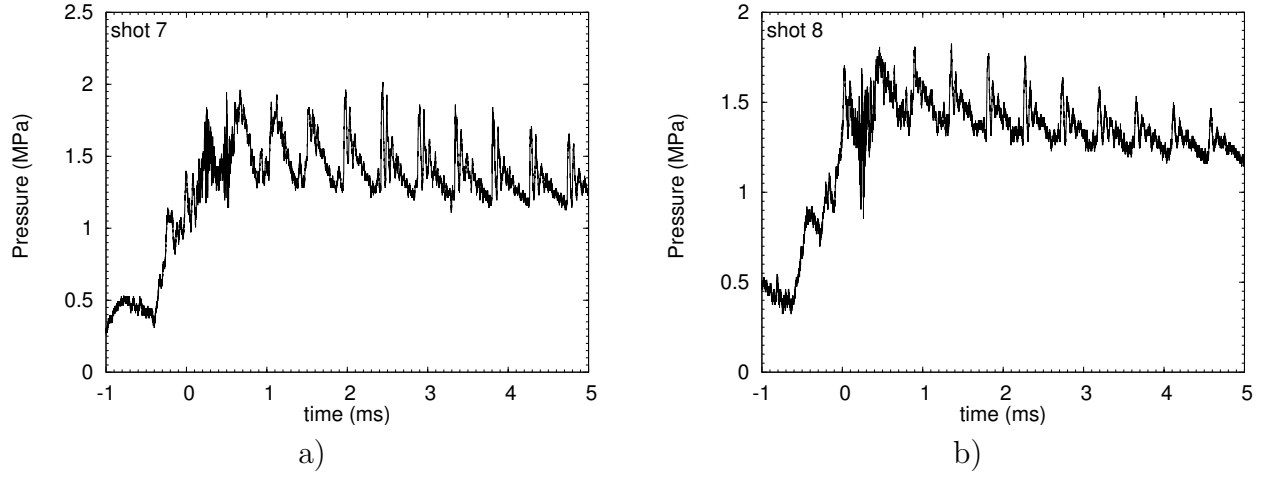


Figure 6: Pressure traces of a) shot 7 and b) shot 8 for $P_0 = 2.0$ bar.

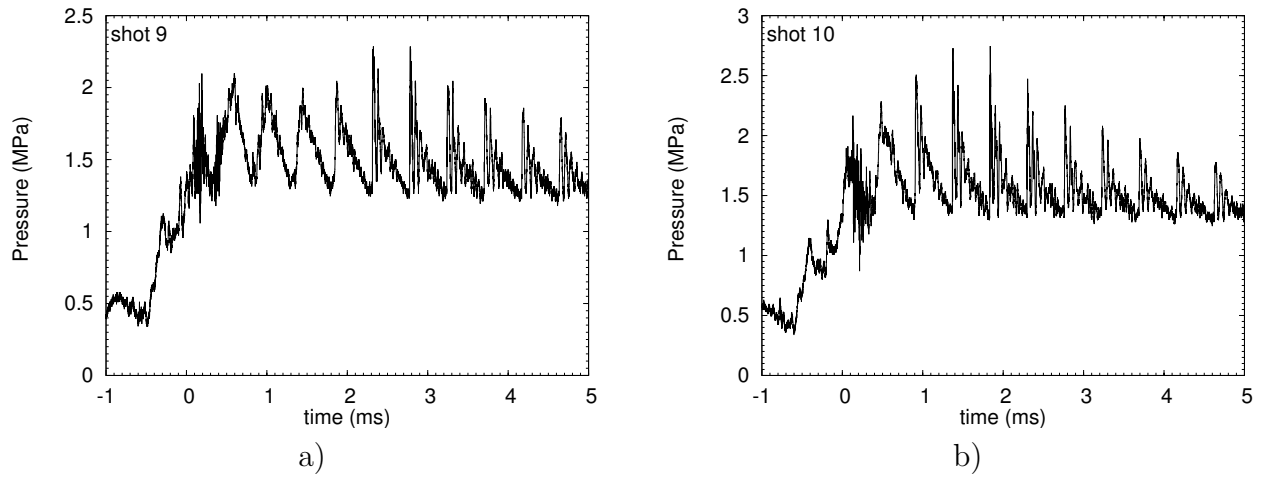


Figure 7: Pressure traces of a) shot 9 for $P_0 = 2.15$ bar and b) shot 10 for $P_0 = 2.2$ bar.

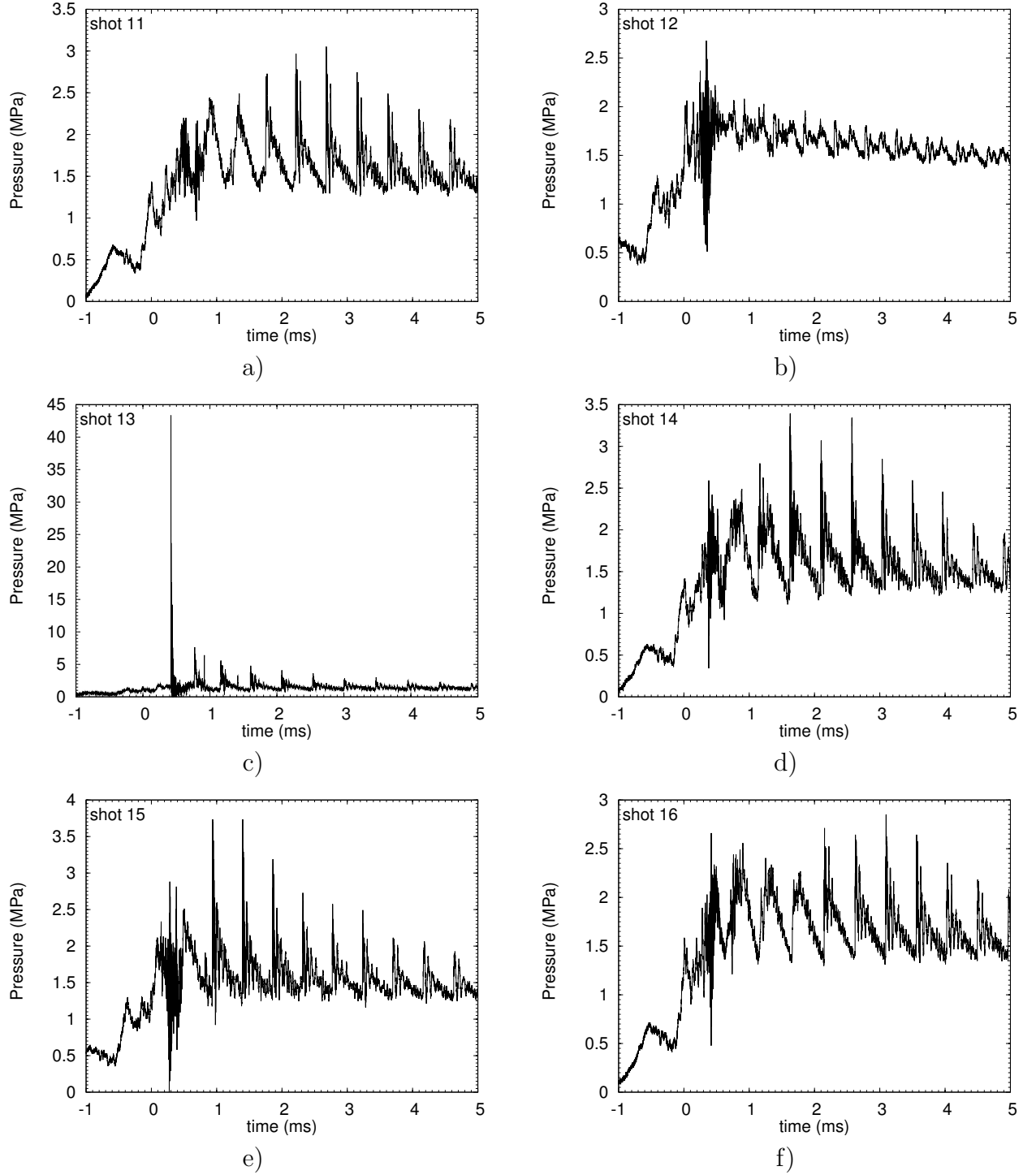


Figure 8: Pressure traces of a) shot 11, b) shot 12, c) shot 13, d) shot 14, e) shot 15 and f) shot 16 for $P_0 = 2.3$ bar.

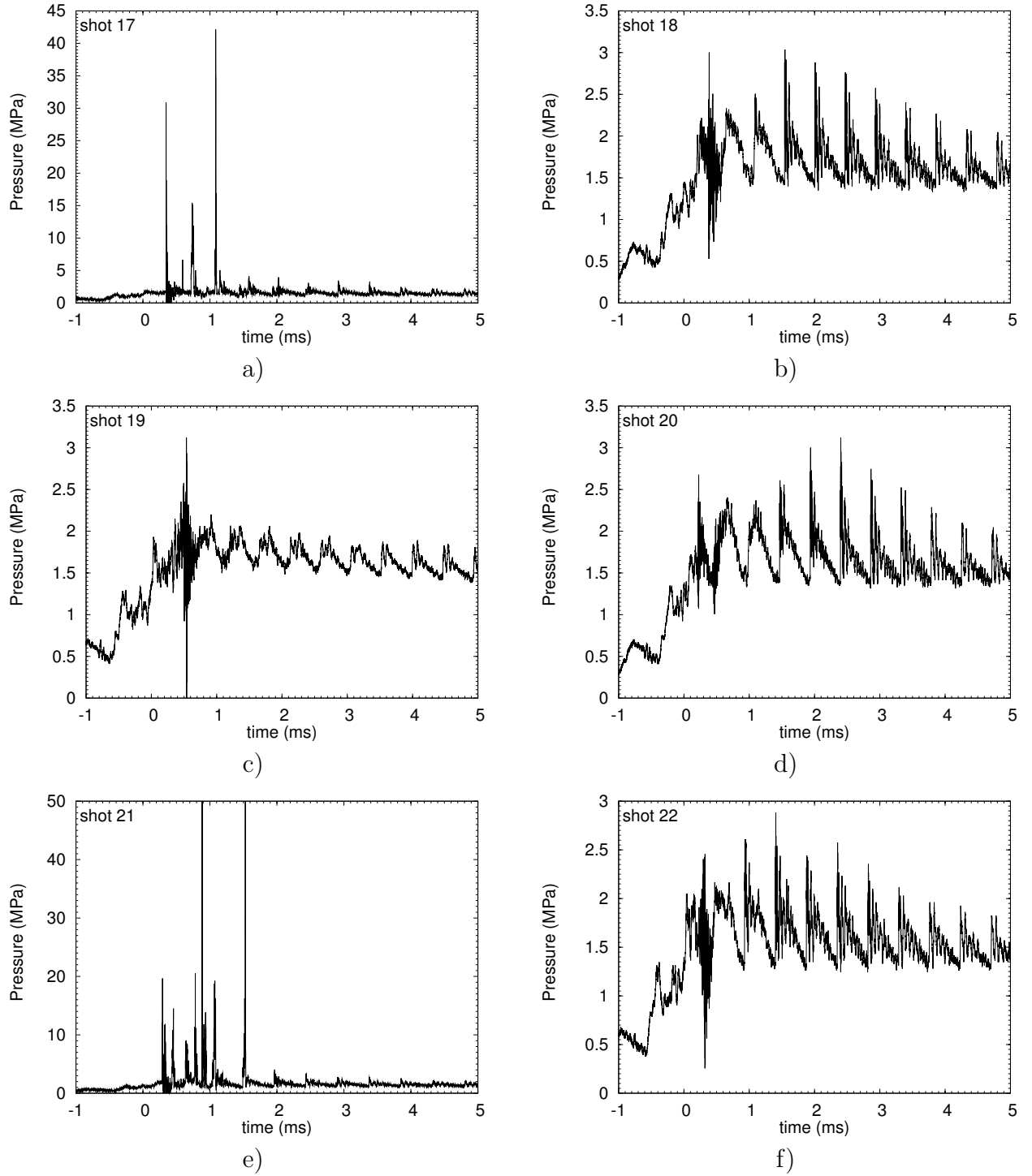


Figure 9: Pressure traces of a) shot 17, b) shot 18, c) shot 19, d) shot 20, e) shot 21 and f) shot 22 for $P_0 = 2.35$ bar.

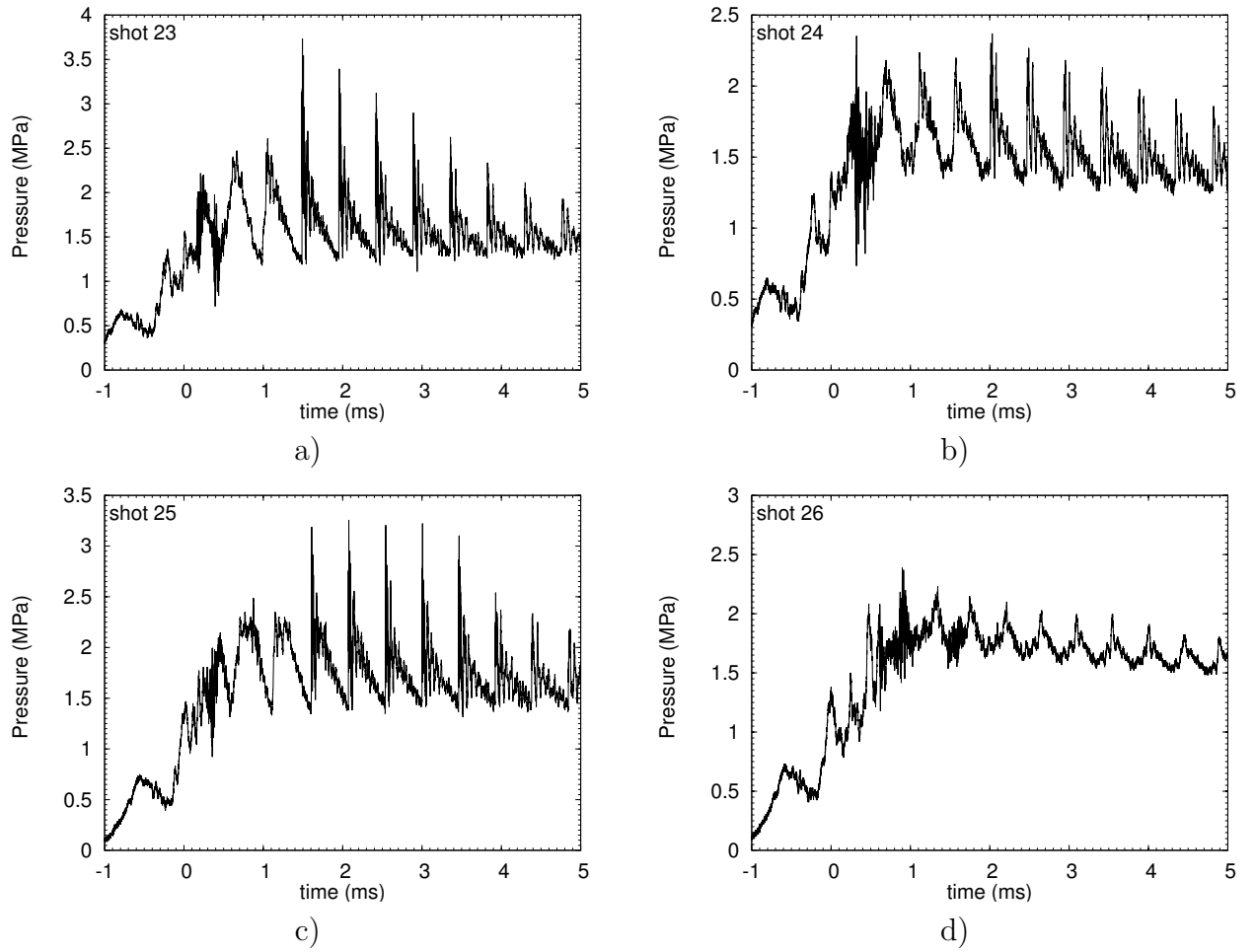


Figure 10: Pressure traces of a) shot 23, b) shot 24, c) shot 25 and d) shot 26 for $P_0 = 2.35$ bar.

B Strain Gauge Traces

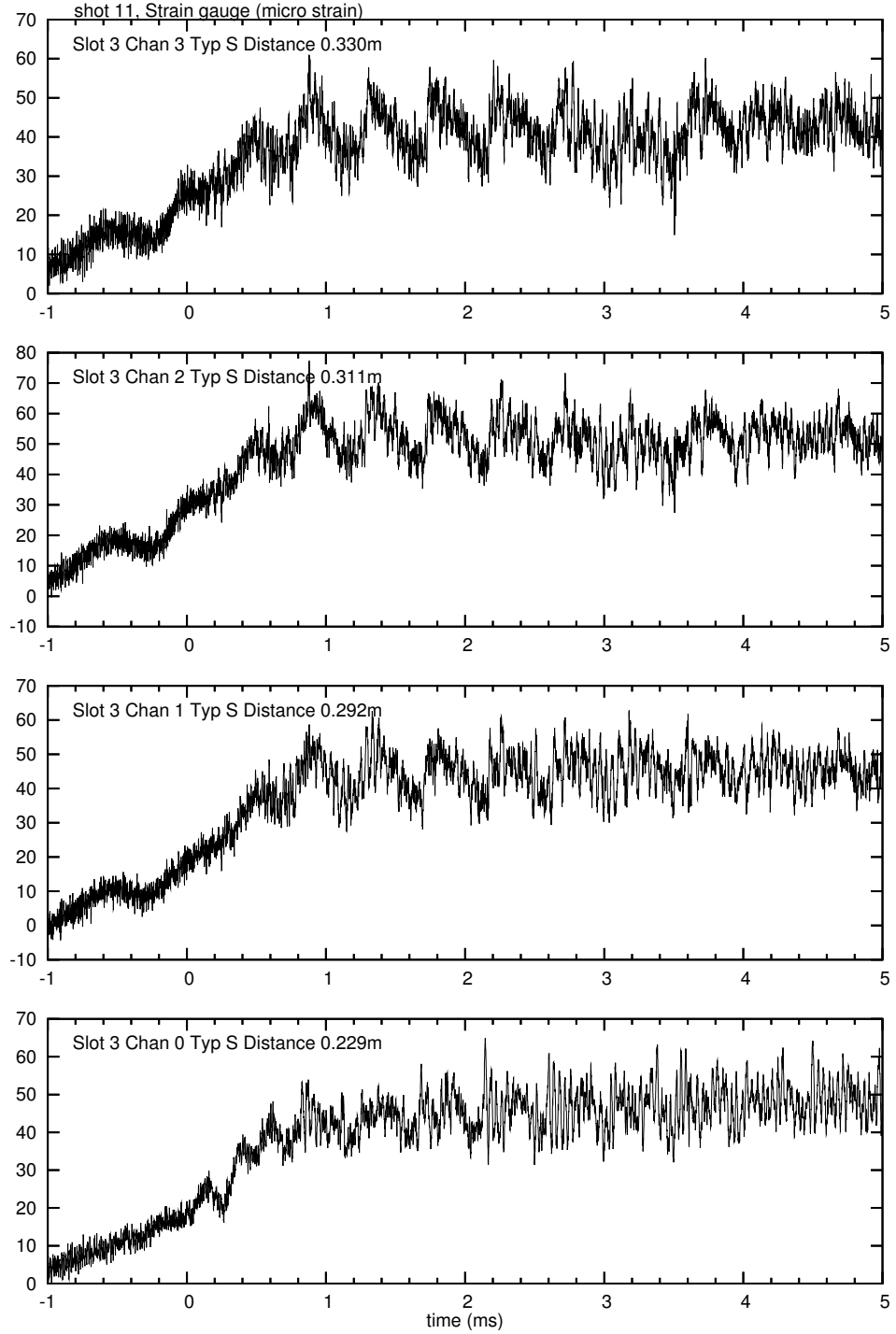


Figure 11: Strain gauge trace of shot 11 for $P_0 = 2.3$ bar.

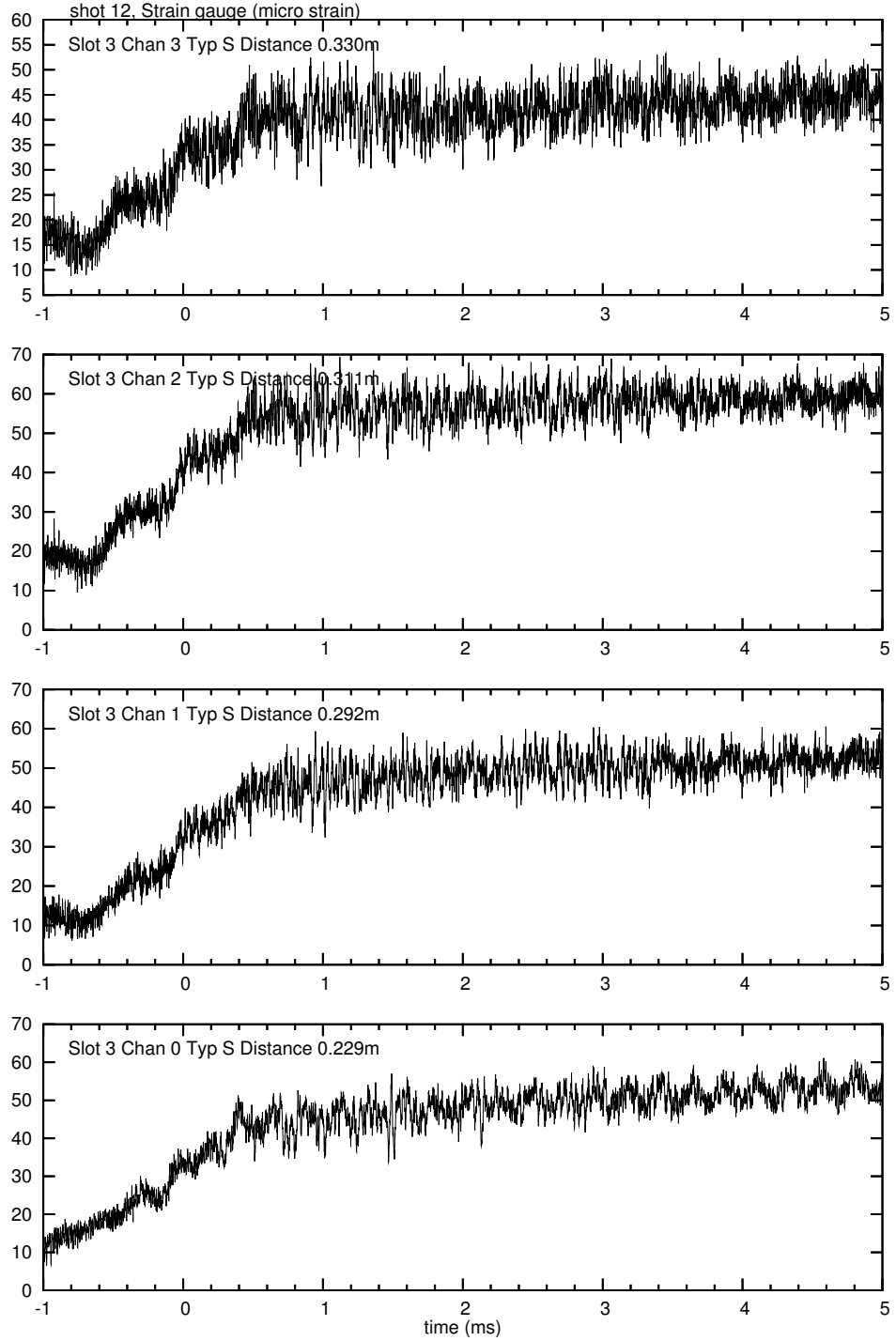


Figure 12: Strain gauge trace of shot 12 for $P_0 = 2.3$ bar.

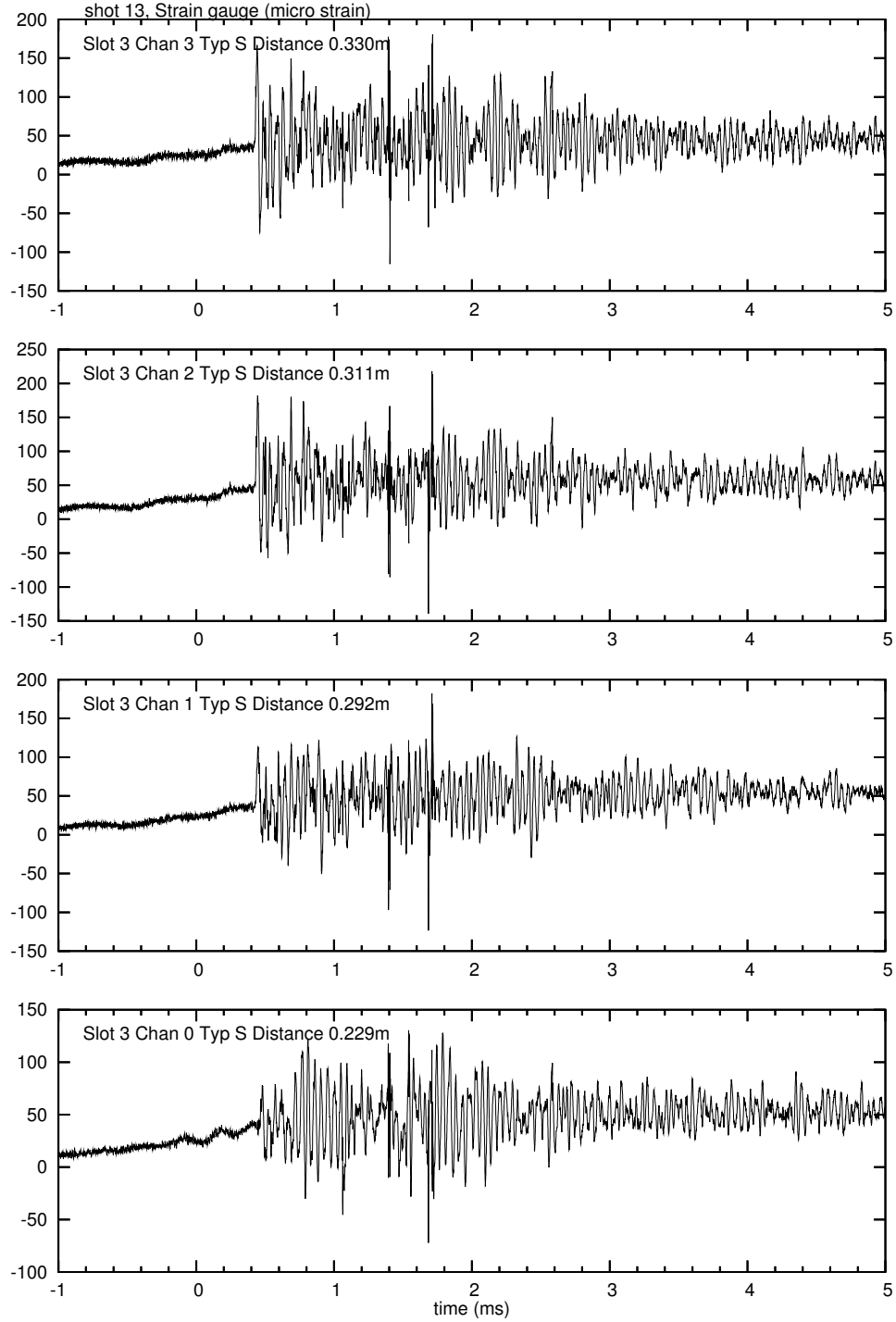


Figure 13: Strain gauge trace of shot 13 for $P_0 = 2.3$ bar.

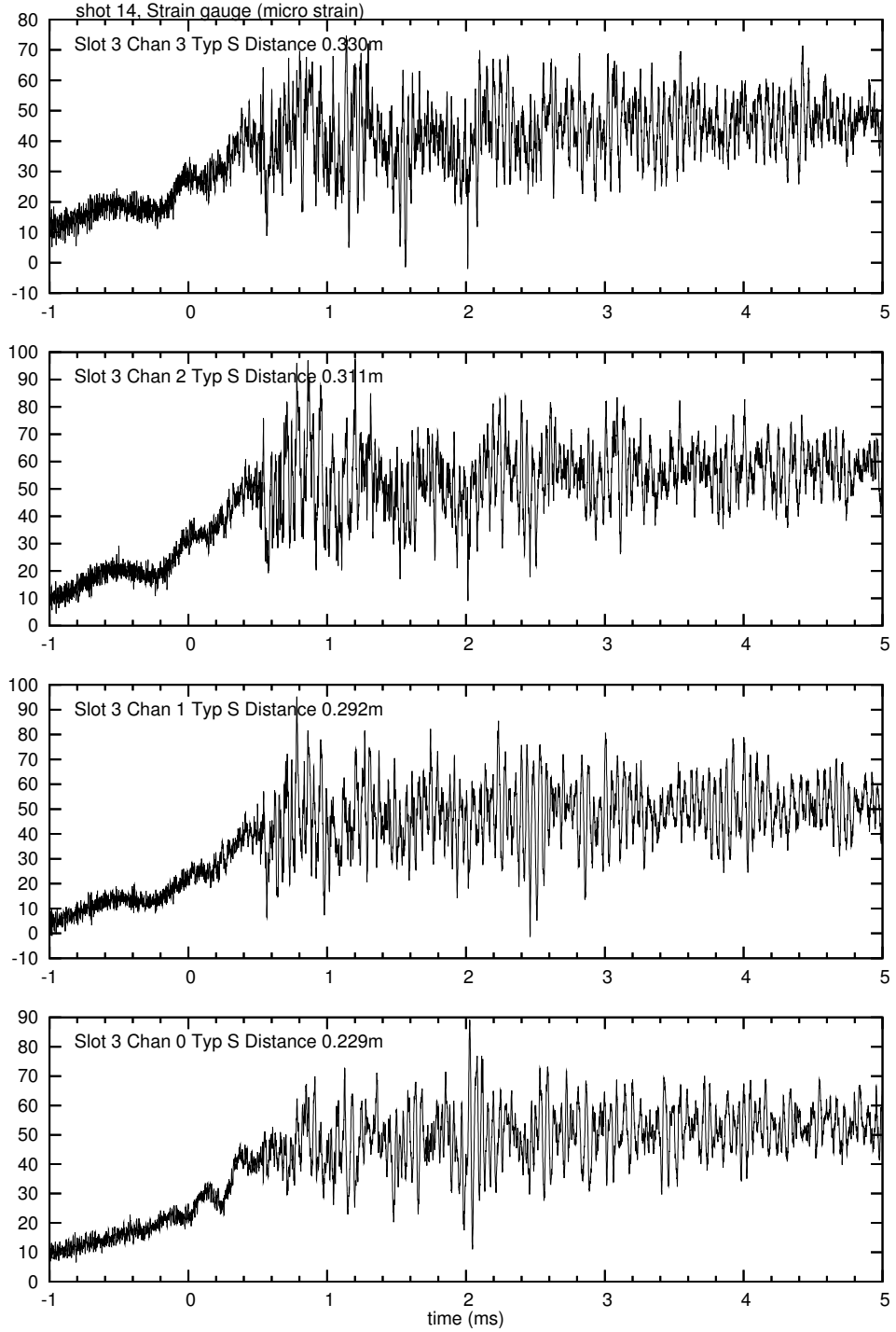


Figure 14: Strain gauge trace of shot 14 for $P_0 = 2.3$ bar.

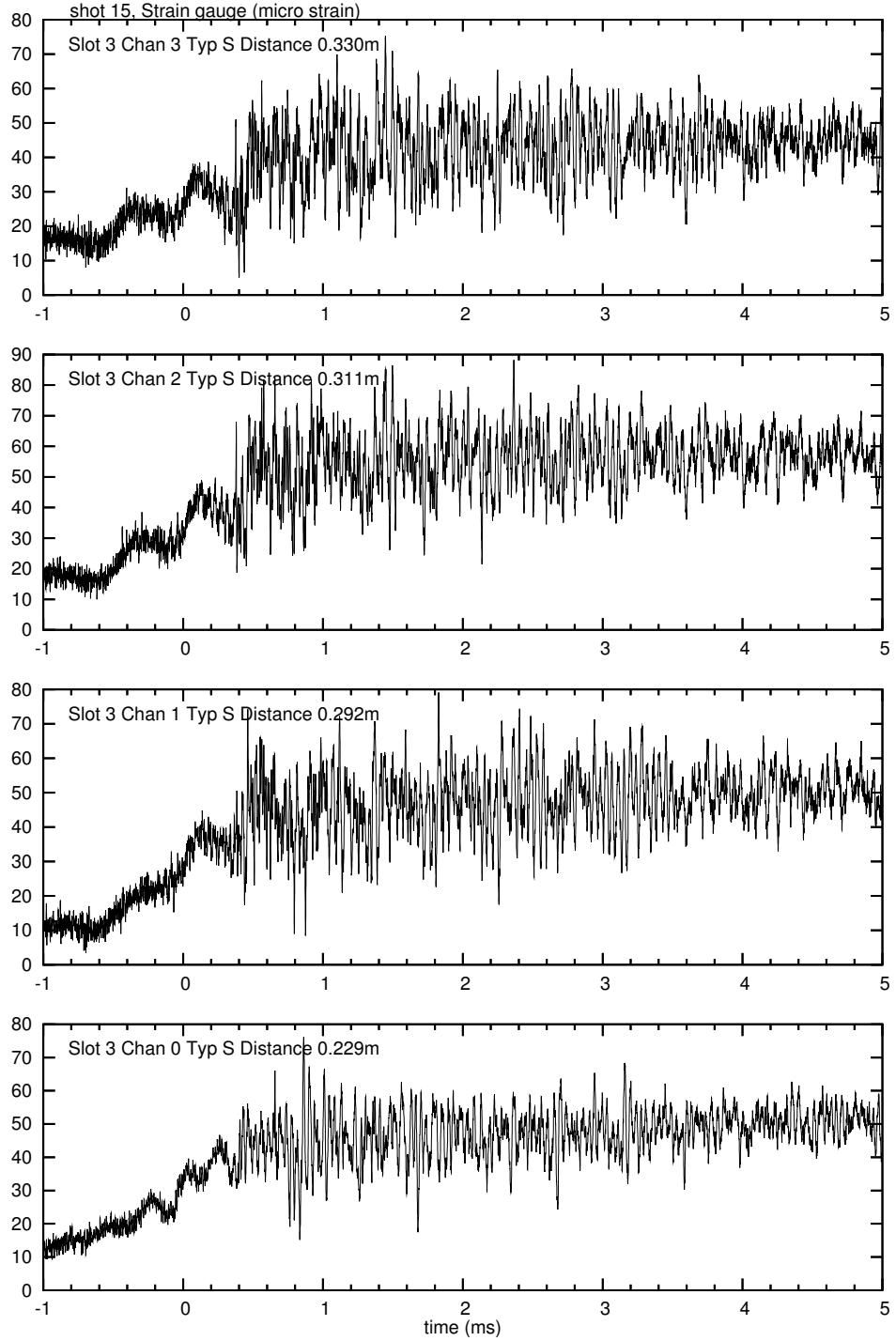


Figure 15: Strain gauge trace of shot 15 for $P_0 = 2.3$ bar.

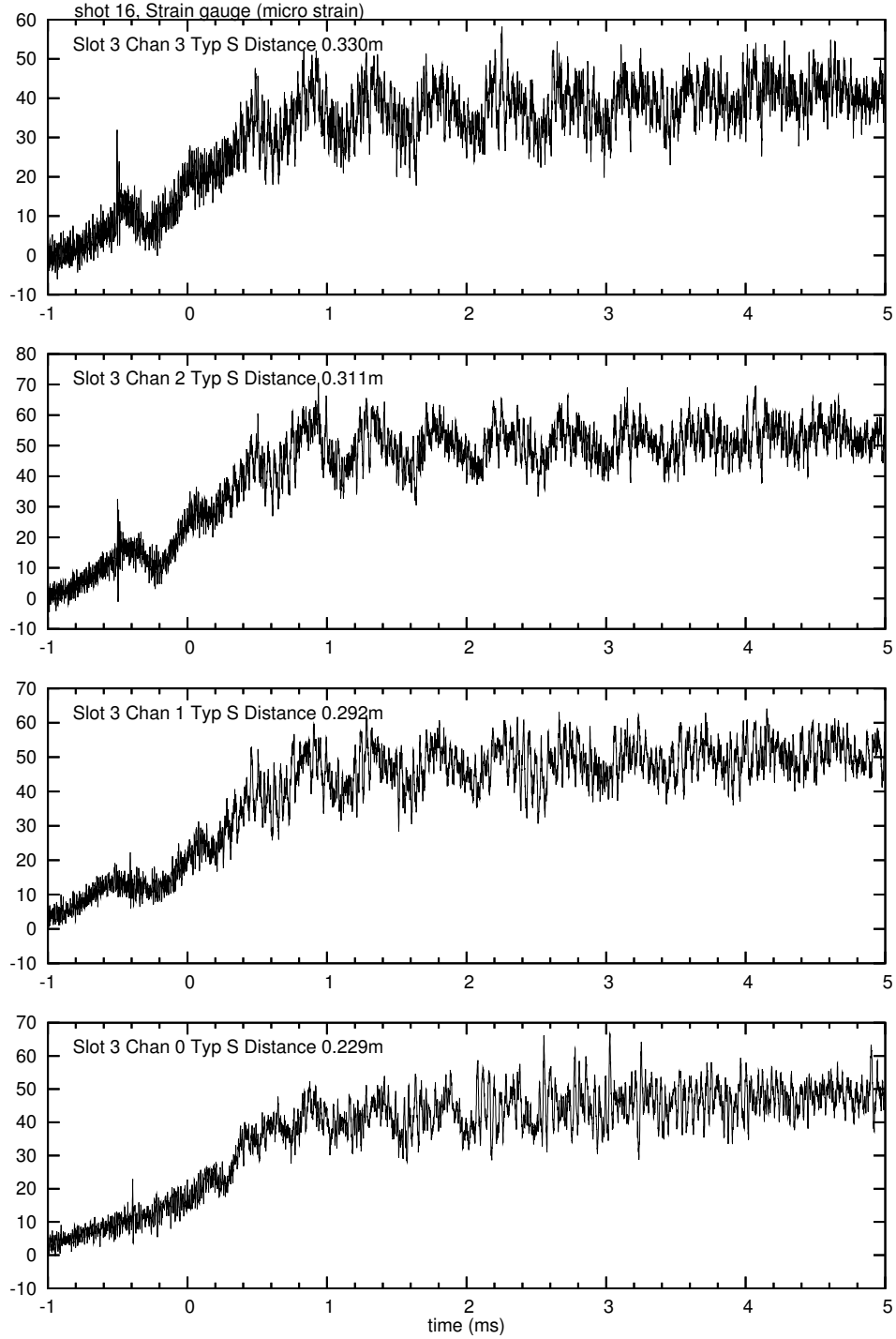


Figure 16: Strain gauge trace of shot 16 for $P_0 = 2.3$ bar.

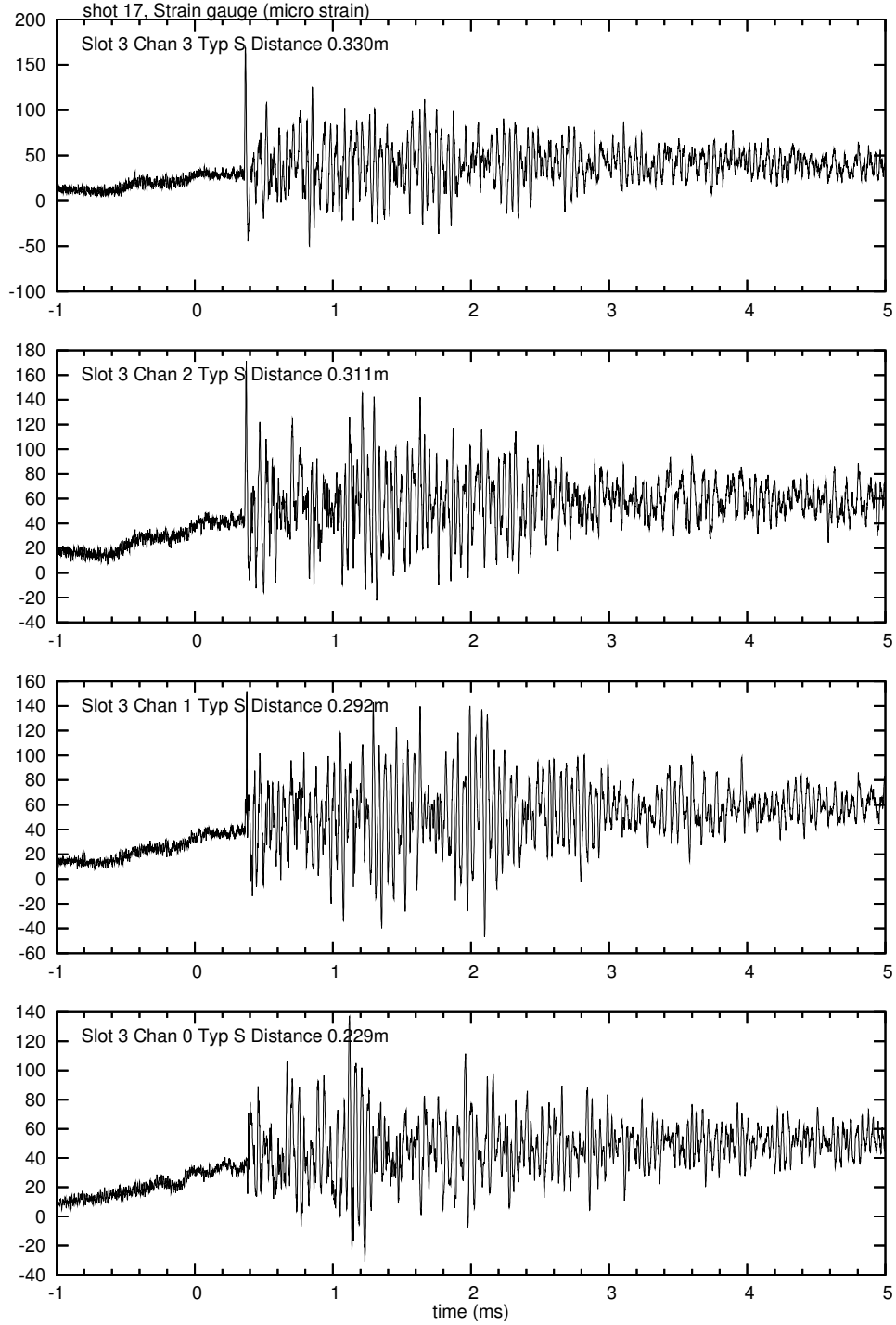


Figure 17: Strain gauge trace of shot 17 for $P_0 = 2.35$ bar.

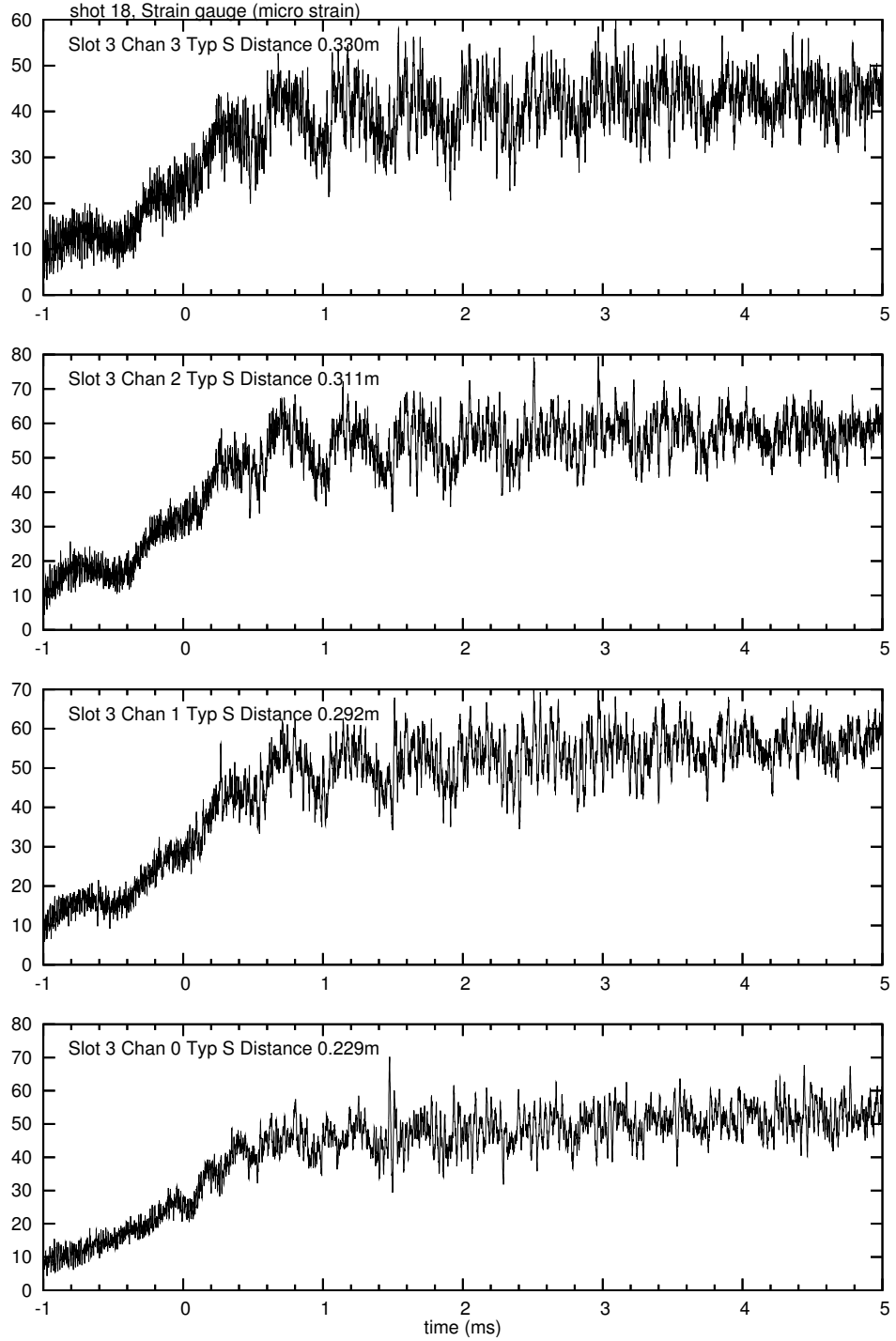


Figure 18: Strain gauge trace of shot 18 for $P_0 = 2.35$ bar.

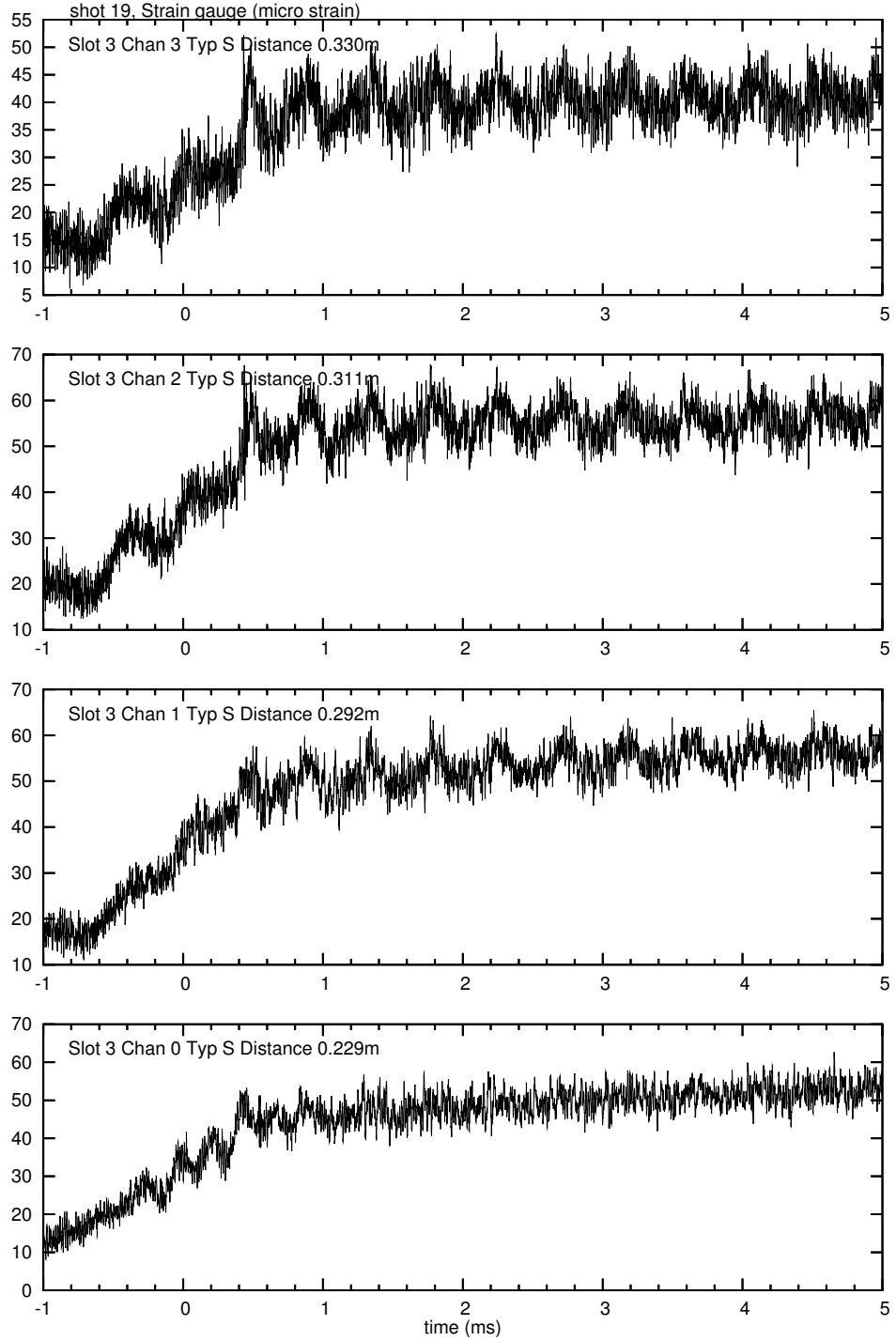


Figure 19: Strain gauge trace of shot 19 for $P_0 = 2.35$ bar.

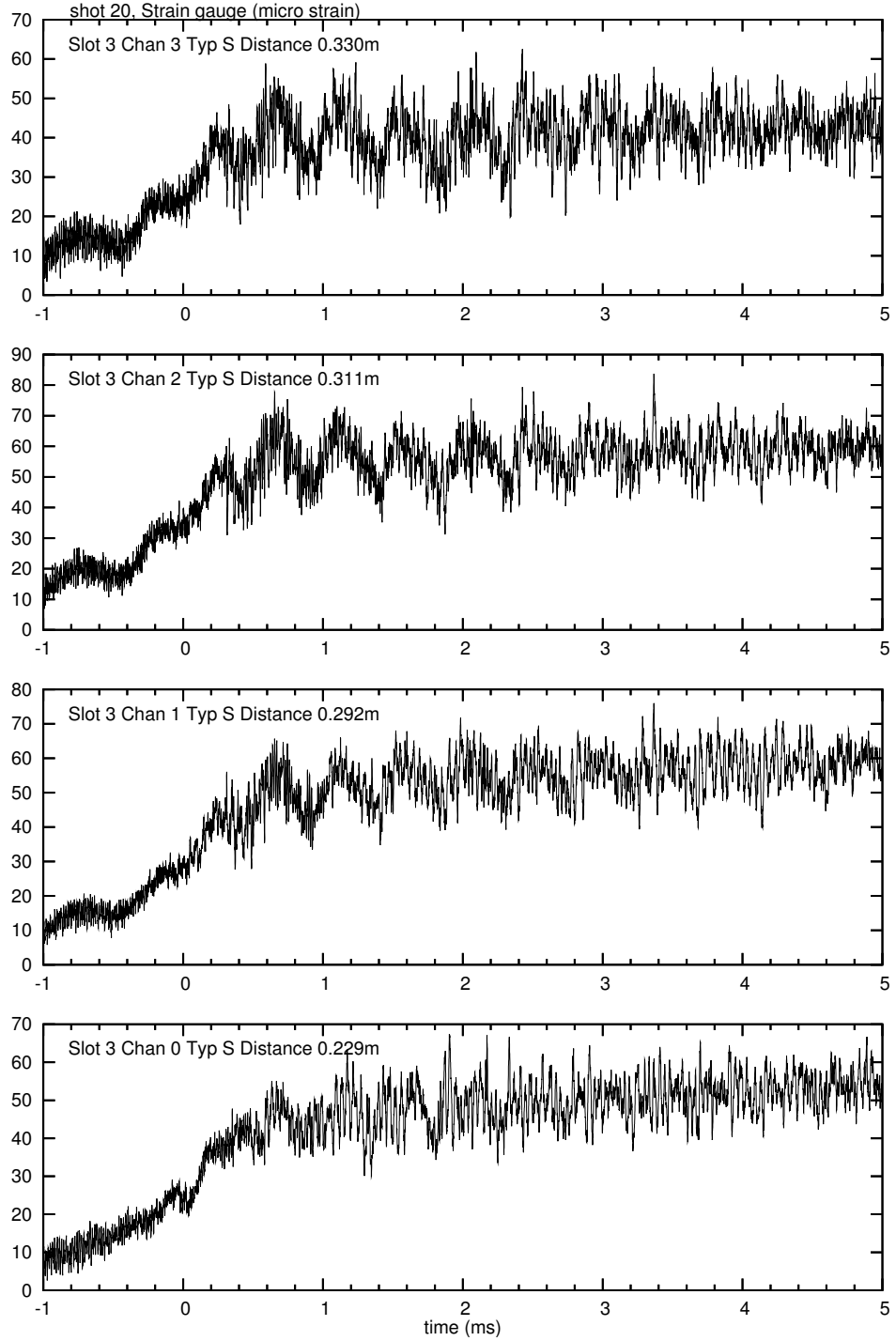


Figure 20: Strain gauge trace of shot 20 for $P_0 = 2.35$ bar.

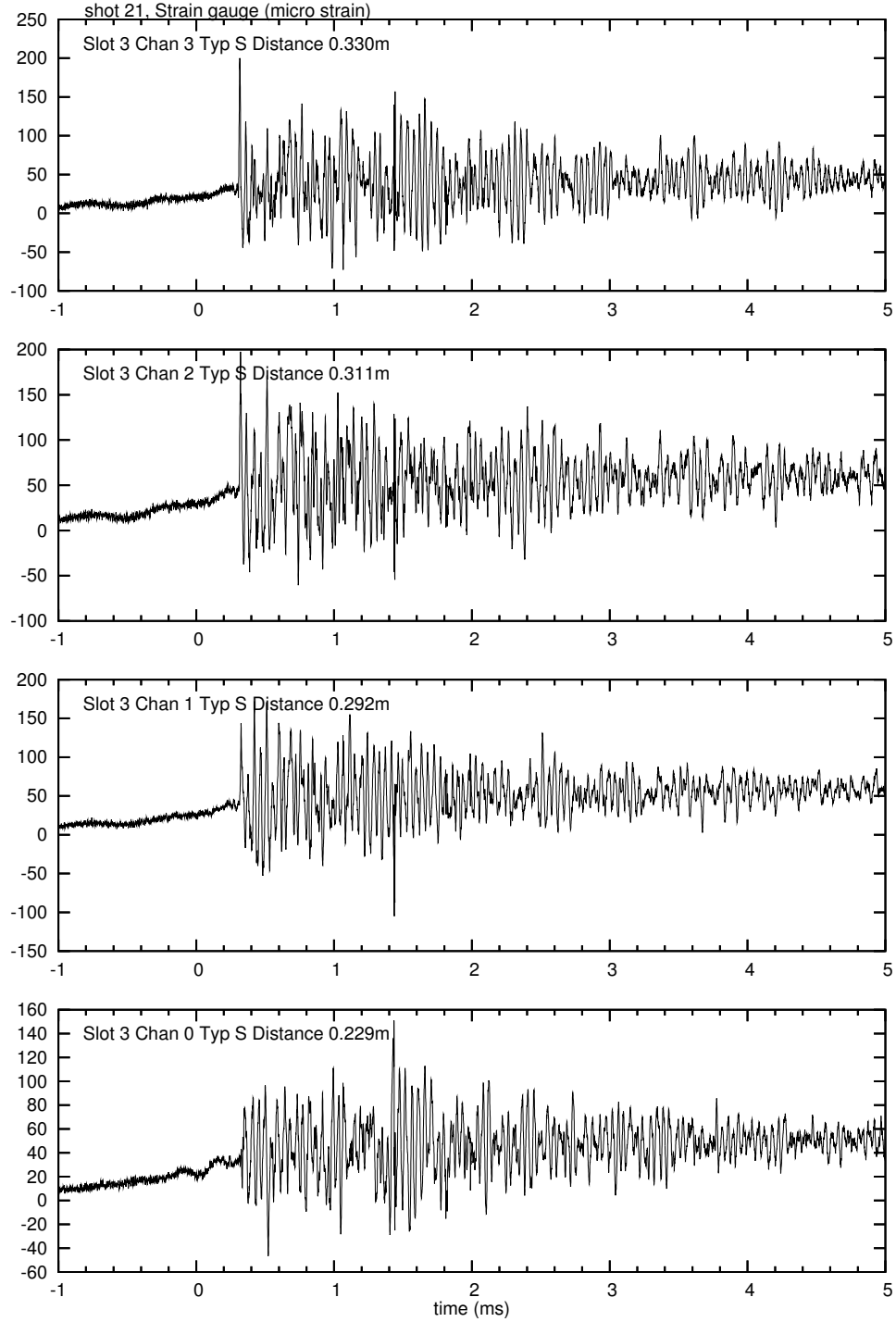


Figure 21: Strain gauge trace of shot 21 for $P_0 = 2.35$ bar.

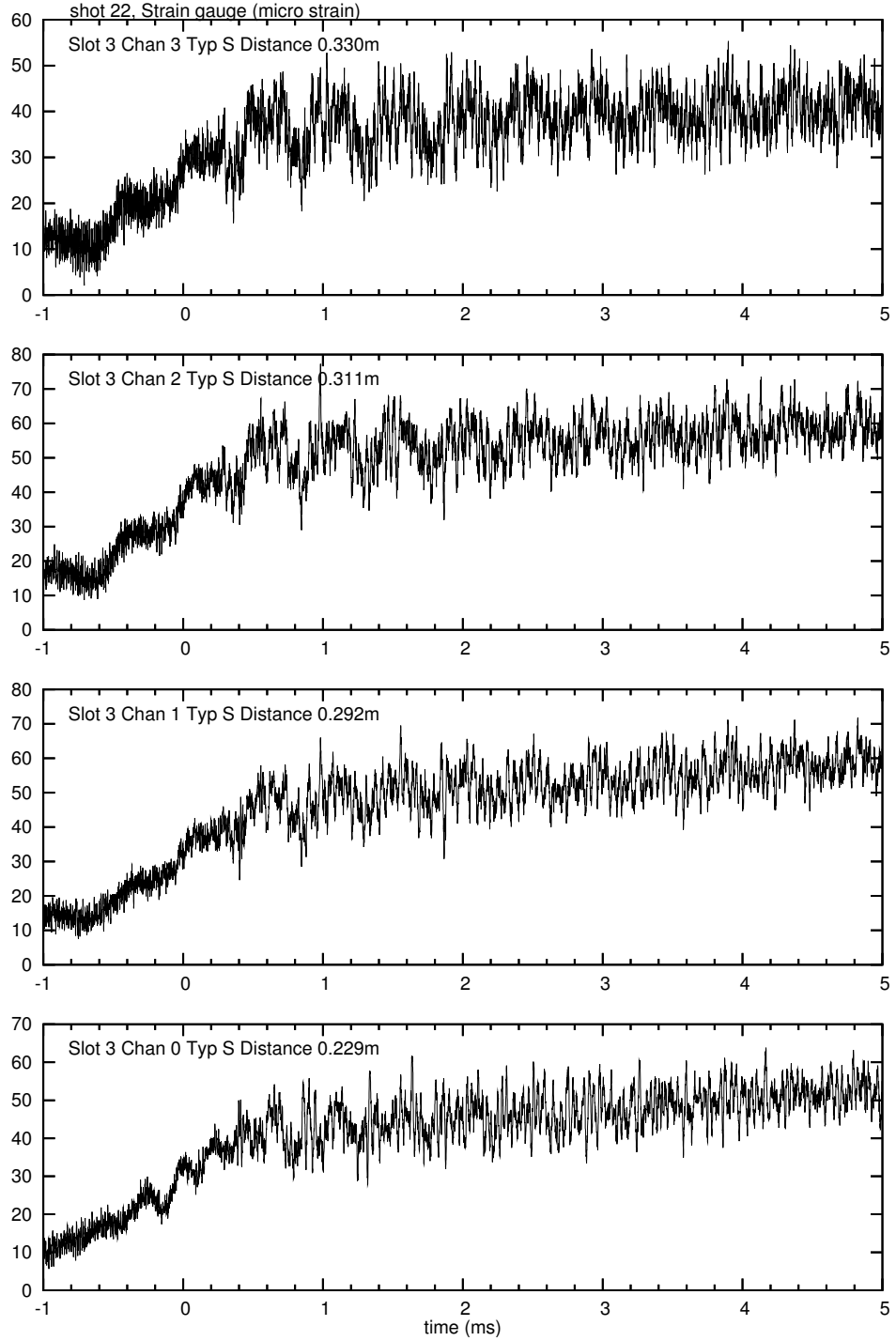


Figure 22: Strain gauge trace of shot 22 for $P_0 = 2.35$ bar.

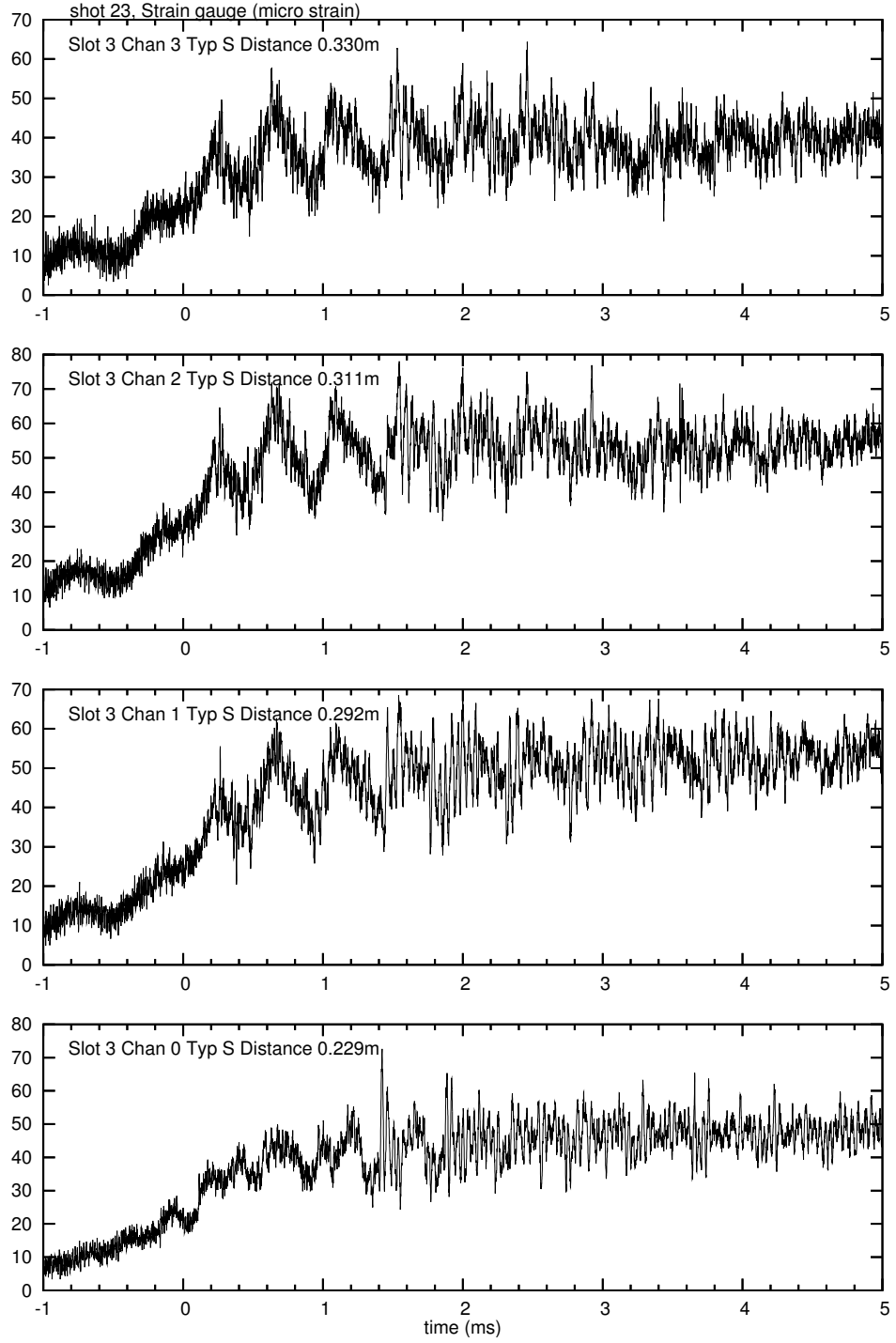


Figure 23: Strain gauge trace of shot 23 for $P_0 = 2.35$ bar.

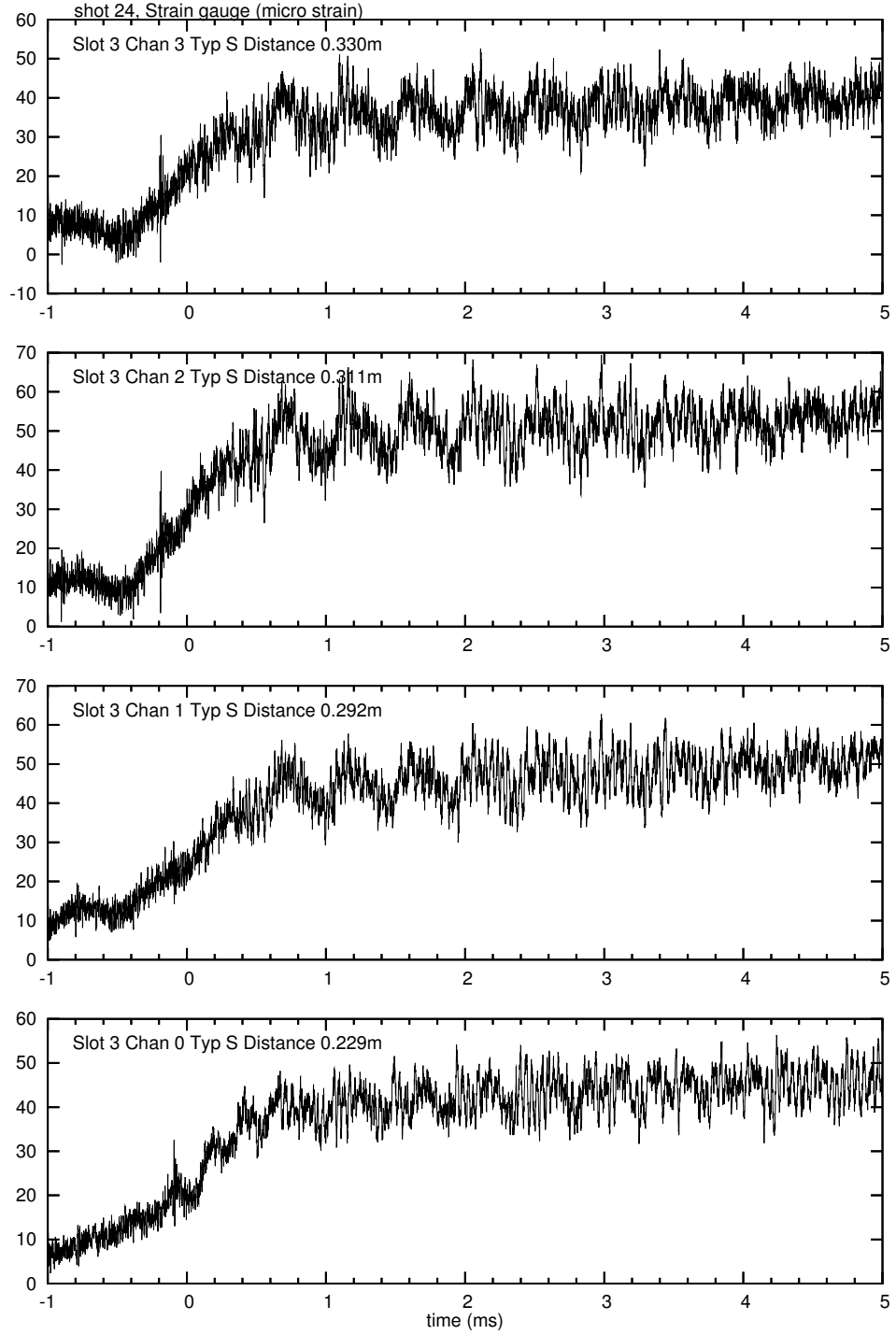


Figure 24: Strain gauge trace of shot 24 for $P_0 = 2.35$ bar.

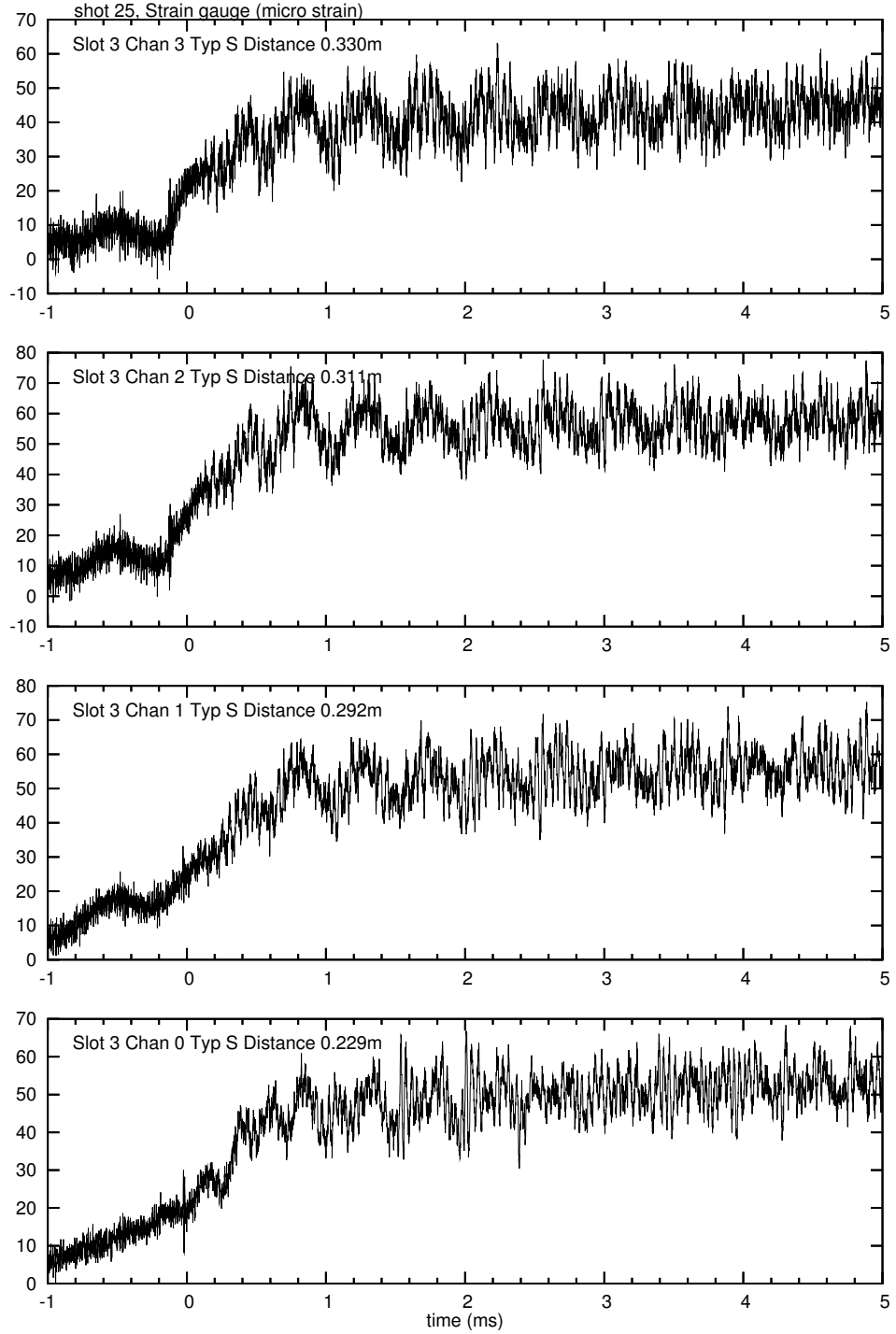


Figure 25: Strain gauge trace of shot 25 for $P_0 = 2.35$ bar.

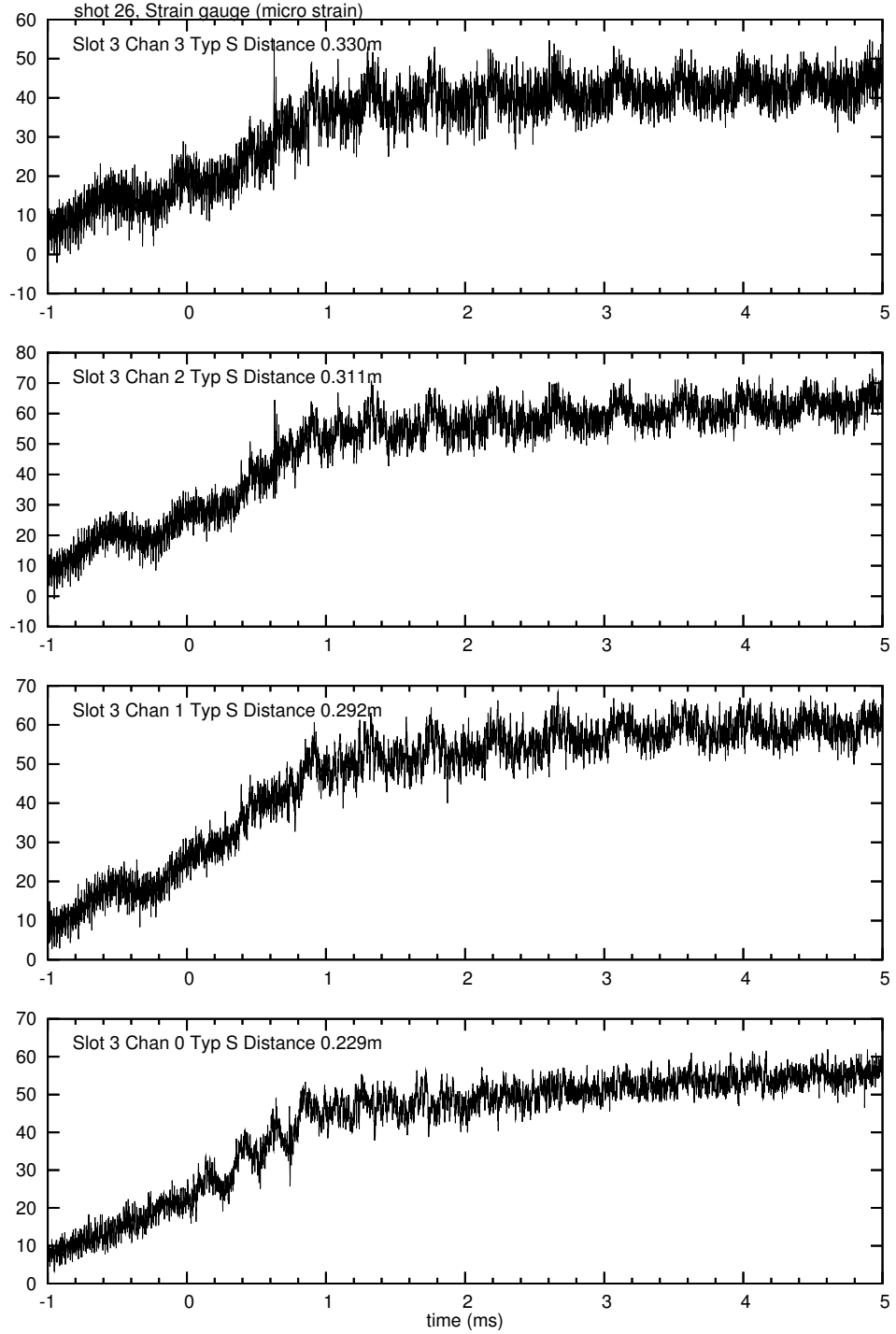


Figure 26: Strain gauge trace of shot 26 for $P_0 = 2.35$ bar.